

Effect of Holding time on performance of extrusion-based 3D printed Calcia Ceramic Core

Bo-lin HU^{1,2}, Ying-peng MU^{1,2}, *Fu-chu LIU^{1,2,3}, Yong-kun XU¹, Zi-tian FAN³

 $(1. School\ of\ Mechanical\ Engineering\ and\ Electronic\ Information, China\ University\ of\ Geosciences,\ Wuhan\ 430074,\ Hubei,\ China;$

2. Shenzhen Research Institute, China University of Geosciences, Shenzhen 51805, Guangdong, China;

3.State Key Laboratory of Materials Processing and Die & Mould Technology, School of Materials Science and Engineering, Huazhong University of Science and Technology, Wuhan, 430074, China)

*Corresponding author: e-mail addresses: liufuchu@cug.edu.cn (Fuchu Liu)

Abstract: The ceramic slurry was prepared using calcium carbonate powder as the matrix material and polyethylene glycol aqueous solution as the binder, slender ceramic core green bodies were fabricated by micro-extrusion 3D printing forming technology, and then water-soluble calcia ceramic cores for casting were obtained by stepwise sintering process. The effects of air sintering, half-embedded and fully-embedded sintering methods of industrial alumina powder on the morphology and properties of cores were investigated. The results show that Insulation time has no effect on the deformation of elongated calcium oxide ceramic core and cracks, with the increase of insulation time, the bulk density of the ceramic core first increases and then remains unchanged, but the insulation time is too long will cause shrinkage and deformation of the amount increases. When fully buried sintering is used, the sintering temperature is 1300 °C, the heating rate is 2 °C/min, and the holding time is 2 h, the core has no cracks, the sintering deformation is 0.11 mm, the linear shrinkage rate is 10.67 %, the bending strength is 4.96 MPa, and the water solubilization rate is 4.4 g/s·m², which is a good overall performance.

Keywords: calcia ceramic core; micro-extrusion 3D printing forming technology; holding time; sintering deformation; rapid casting

1 Introduction

With the growing demand for complex structures, lightweight and precision castings in the field of high-end equipment manufacturing, such as aero-engine blades, spacecraft components, high-speed rail brake discs and other key components, the internal cavity structure is gradually developed in the direction of thin-walled, complex and integrated^[1-2]. The manufacturing of such castings relies on the traditional investment casting process, the core of which is to accurately form the complex internal cavity structure through ceramic cores^[3]. However, the traditional ceramic core preparation process relies on mold forming, and there are bottlenecks such as low design freedom, long development cycle, and high cost of modification, which makes it difficult to adapt to the rapid iteration of customized production

they are difficult to be de-cored and the process is complicated^[10-12]; MgO-based ceramic cores are outstanding in high-temperature resistance and thermal shock resistance, but the problem of hygroscopic

requirements^[3-5].In the 21st century, 3D printing technology, with the characteristics of mold-less, layer-by-layer molding, has provided a subversive solution for the efficient preparation of complex ceramic cores^[6].

According to the different matrix materials, the commonly used ceramic cores can be divided into SiO₂-based ceramic cores, Al₂O₃-based ceramic cores, MgO-based ceramic cores, and CaO-based ceramic cores^[7]. SiO₂-based ceramic cores are widely used due to low cost, easy to remove the core, etc., but their high-temperature strength is insufficient and easy to react with the metal liquid, which limits their application in the alloys^[8-9]; high-temperature casting of Although Al₂O₃-based ceramic excellent cores have high-temperature stability and mechanical properties, chalking has not yet been solved[13-14]; CaO-based ceramic cores are widely used because of their high melting point (2572°C), excellent thermomechanical stability and post-casting water-soluble properties^[11]. CaO-based ceramic cores are regarded as ideal candidates for complex high-temperature castings due to their high melting point (2572°C), excellent thermomechanical stability, and post-casting water-soluble removal properties^[15-17].

Micro-extrusion 3D printing is formed through filament-by-filament and layer-by-layer stacking, and the slurry between adjacent layers is prone to form microscopic interfacial defects due to the extrusion pressure, differences in rheological properties, and non-synchronization of curing rates^[18-19], and these defects expand into macroscopic cracks due to the localized stress concentration at the sintering stage^[20]. This limits the wide application of 3D printing technology for complex CaO ceramic cores.

The method of buried powder sintering plays an effective role in suppressing ceramic sintering cracking and deformation.Li et al^[21] buried light-curing 3D printed alumina ceramic cores into different particle sizes of alumina powder for sintering, and the results showed that with the increase of the buried powder particle size from 5 μm to 1,000 μm, the ceramic shrinkage, density, and flexural strength increased, while the open porosity was reduced, and the optimal buried powder size was 1,000 μm, and the buried powder was 1,000 μm, which is favorable for balancing the stress in the green body. The optimal buried powder particle size is 1000 µm, the buried powder sintering is conducive to balancing the stress within the green body, and the volatilization of photosensitive resin compensates for the vapor pressure of the external environment, which can effectively reduce the deformation of ceramics and improve their performance. Huang et al^[22] improved the mechanical properties of composite ceramic green bodies by burying the boron powder-assisted sintering, and the results show that the buried boron powder sintering effectively inhibits the decomposition of ceramic green bodies reduces the grain size and significantly improves the ceramic hardness and relative density. hardness and relative density.

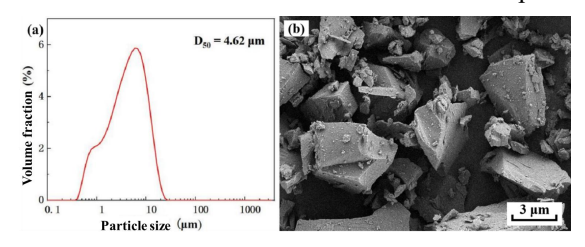
For this reason, in this paper, the ceramic slurry is prepared with calcium carbonate powder as the matrix material and polyethylene glycol aqueous solution as the binder, and the ceramic core green bodies are prepared by micro-extrusion 3D printing technology. Using air sintering, half-embedded and fully-embedded sintering of industrial alumina powder, the influence of holding time on the properties of elongated CaO ceramic cores, such as morphology, sintering deformation, bending strength, and water solubility rate, etc., was investigated, and the

optimized sintering strategy of water-soluble CaO ceramic cores was determined, and the deformation mechanism of elongated CaO ceramic cores in the process of sintering was analyzed, so that elongated water-soluble CaO ceramic cores with low shrinkage and deformation could be prepared. CaO ceramic cores with low shrinkage and low deformation were prepared.

2 Experimental section

2.1 Raw materials

In this study, 1 250 mesh CaCO₃ powder (D50=4.62 μm, Changzhou Yuanxin Materials Technology Co., Ltd., China) was used as the matrix material, and the particle size and microscopic morphology of the particles are shown in Fig. 1. Polyethylene glycol (PEG, Mw=4 000 g/mol, China National Pharmaceutical Group Chemical Reagent Co., Ltd.) solution with a mass fraction of 30 wt.% was configured with deionized water as the solvent as the binder, and organosilicone antifoam (BYK-066N, Wuhan Joyan Science and Technology Co., Ltd.) was used in order to remove air bubbles from ceramic pastes.



(a)particle size distribution (b)microscopic morphology

Fig. 1 Properties of calcium carbonate powder

2.2 Preparation of ceramic cores

The preparation process of ceramic core samples mainly includes ceramic slurry preparation, micro-extrusion 3D printing process and heat treatment process (drying and sintering), and the schematic diagram of the micro-extrusion 3D printing process is shown in Fig. 2.

Calcium carbonate powder was added to the PEG aqueous solution with manual mixing until initial dispersion, and 0.5% silicone defoamer was added to remove air bubbles in the slurry, and finally the mixed slurry was transferred to a planetary ball mill (QM-QX, Nanjing Laibu Science and Technology), and ball milled at a speed of 300 r/min for 9 h. The composition of its slurry is shown in Table 1.

Tab. 1 CaO Ceramic Paste Components

Slurry Composition	Quantity(g)
CaCO ₃	147.34
PEG solution	48.88
Silicone antifoam agent	1

The ceramic slurry after ball milling was injected the extrusion barrel of the laboratory's into self-developed micro-extrusion 3D printing device, installed the appropriate needle and loaded into the printer, using Simplify 3D software to set the printing parameters^[23]. The length, width and height of the prepared slender ceramic green bodies were 120 mm, 6 mm and 2 mm, respectively, and the ceramic green bodies were self-hardened at room temperature and then moved to the drying oven (DZF-6030, Shanghai Jinghong Experimental Equipment Co., Ltd.) with a set temperature of 70 °C for 24 h. After drying, the green bodies were placed in a high-temperature sintering furnace (YMG1600-40, Shanghai Yanwu Science and Technology Co., Ltd.) for sintering. After drying, the green bodies were placed in a high temperature sintering furnace (YMG1600-40, Shanghai Yanwei Technology Co. At the end of sintering, the ceramic core was naturally cooled to room temperature to obtain the elongated CaO ceramic core.

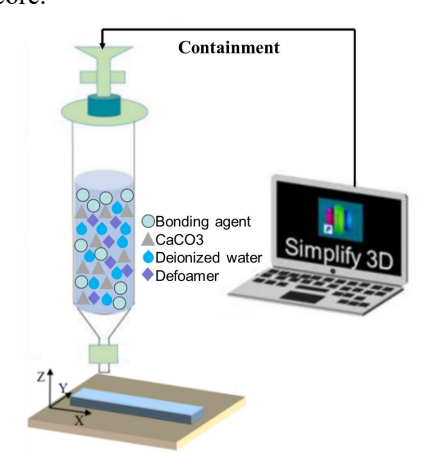


Fig. 2 Schematic of Direct Ink Writing (DIW) 3D priting

2.3 Sintering process program

Sintering, as a key link in the preparation process of ceramic cores, the core mechanism is to promote the formation of strong chemical bonding between particles through high-temperature heat treatment to effectively reduce the porosity of the material, which significantly improves the degree of densification of ceramic cores and their mechanical property indexes^[24-25].

Three sintering methods were selected for the study: air sintering^[26-29], semi-buried sintering^[30,31] and fully buried sintering^[32,33]. Among them, 200 mesh white corundum was used for the buried powder sintering. Air sintering involves placing the ceramic cores directly in a sintering furnace for heating, which is a simple method but may lead to oxidization and

deformation of the ceramic cores. Semi-embedded sintering involves partially burying the ceramic core in the powder, utilizing the cushioning effect of the powder to minimize thermal stress and reduce the risk of cracking. Fully buried sintering involves burying the entire ceramic core in the powder to achieve more uniform heat transfer and more effective thermal stress control. The three sintering processes are shown in Fig. 3.

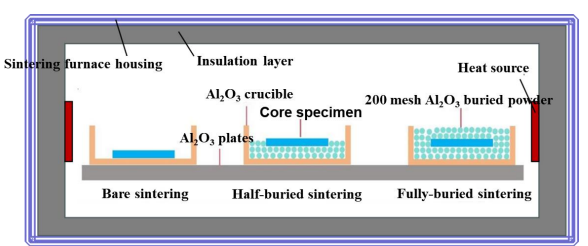


Fig. 3 Schematic diagram of different sintering methods for CaO ceramic cores

Our research team has previously tested the thermogravimetric analysis of the completely dried ceramic coregreen bodies^[15], and the ceramic core green bodies showed two significant mass loss stages during the heat treatment process: at 200 °C, which was mainly attributed to the thermal decomposition and volatilization of physically adsorbed water and PEG; and at 750 °C, which originated from the decomposition of CaCO₃ into CaO and CO₂. Based on this, this study adopts a stepwise sintering process with staged holding times at 200 °C and 750 °C, respectively, to achieve optimized sintering of core green bodies.

The sintering curves of ceramic core green bodies with different holding times are shown in Fig. 4. Under the condition of ensuring the constant heating rate and sintering temperature, the ceramic core specimens were sintered at 200 °C, 750 °C and 1 300 °C with holding times of 1, 2, 3 and 4 h, respectively, where the heating rate was selected to be 2 °C/min, and the final sintering temperature was 1 300 °C.

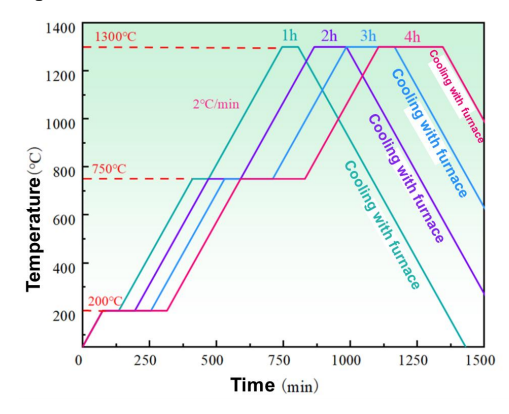
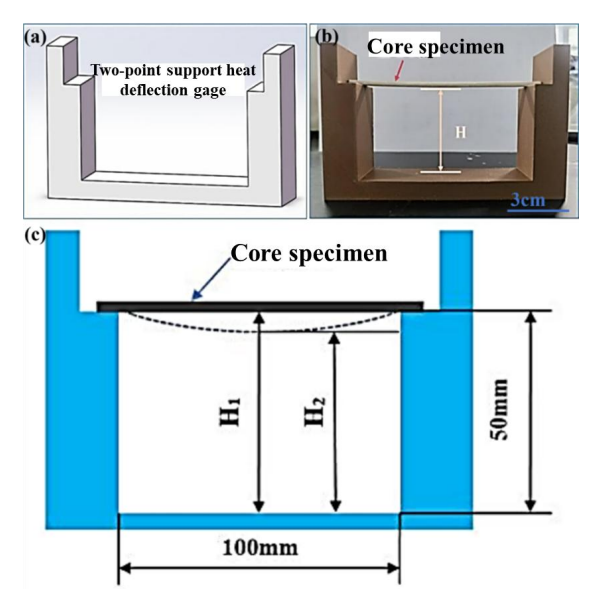


Fig. 4 Sintering curves with different holding times

2.4 Performance Characterization

In order to ensure the reliability of the results, the following macroscopic performance of each group are tested five ceramic core samples and take the average value.

Fig. 5 shows the three-dimensional model of the homemade two-point support gage and the measurement schematic. The high-temperature sintering deformation (ΔH) was measured by the homemade two-point support gage, and was calculated as the height difference between the lowest point of the ceramic core and the bottom of the gage before and after sintering (H_1 - H_2), where H_1 is the height before sintering and H2 is the height after sintering.



(a) Sintering deformation amount of two-point support gage model (b) Physical measurement diagram (c) Measurement diagram

Fig. 5 Sintering deformation of two-point support gauge model and physical measurement

The dimensional changes of the samples before and after sintering were measured using vernier calipers at the three center points of the ceramic cores, length, width and height, respectively, to calculate the linear shrinkage. The flexural strength of the ceramic cores was tested according to the three-point bending method using a universal testing machine (ETM105D-T, Shenzhen Wanji Experimental Equipment Co., Ltd.).

The porosity and bulk density of the ceramic cores were tested using a density balance (LQ-C5003, Shanghai Yaoxin Electronic Technology Co., Ltd.) based on the Archimedes drainage method^[28], and kerosene was chosen as the measurement medium (density of kerosene

at room temperature $\rho 0 = 0.78$ g/cm3) because CaO-based ceramic cores are easily collapsed in water, the mass of the ceramic cores was measured using a density balance (LQ-C5003, Shanghai Yaoxin Electronic Technology Co., Ltd.), and the mass of the ceramic cores was calculated using a density balance. The mass of dry ceramic core in air, the mass of ceramic core saturated with kerosene in air and the mass of ceramic core saturated with kerosene in kerosene are G1, G2 and G3 respectively, the porosity $P_0=(G_2-G_1)/(G_2-G_3)$, the bulk density $\rho=G_1\times\rho_0/(G_2-G_3)$.

The mass change of CaO ceramic cores in a constant humidity flask for 48 h was determined to calculate the moisture absorption rate. The ceramic cores were placed in water at room temperature, and the mass and surface area of the ceramic cores were recorded as m and s. A stopwatch was used to time the collapse time of the ceramic cores, t, and the water solubilization rate of ceramic cores, $K=m/s\times t$. The microscopic morphology and internal structure of the ceramic powders, the 3D-printed molded ceramic green bodies, and the sintered ceramic cores were observed by using a super depth-of-field microscope (RX-100, Ho-Vision Co. Ltd., Japan).

3 Results and discussion

3.1 Surface morphology of ceramic cores

The results and discussion section should be organized using appropriate sub-headings. Use a normal, plain font for text. Do not use field functions. Use tab stops or other commands for indents, not the space bar. Use the table function, not spreadsheets, to make tables. Use the equation editor or MathType for equations.

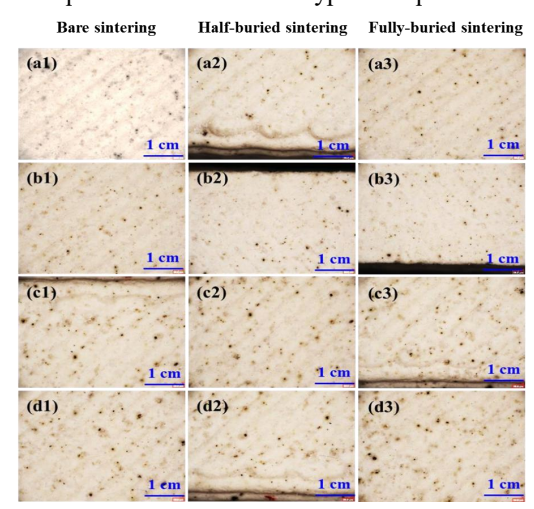


Fig. 6 Surface morphology of ceramic cores sintered at different holding times: (a) 1 h; (b) 2 h; (c) 3 h; (d) 4 h 3.2 Study of sintering properties of ceramic cores

3.2.1 High temperature sintering deformation

The high-temperature sintering deformation of sintered CaO cores at different holding times is shown in Fig. 7. Under the same sintering method when the holding time is increased from 1 h to 3 h, the high-temperature sintering deformation of ceramic cores grows slowly, and the sintering deformation of cores increases sharply from 3 h to 4 h. The sintering deformation of air-sintered cores is shown in Fig. 7. When the holding time increases from 1 h to 3 h, the high-temperature sintering deformation of air-sintered cores increases from 0.68 mm to 0.84 mm, and when the holding time increases from 3 h to 4 h, the high-temperature sintering deformation cores increases from 0.84 mm to 1.6 mm.

When the holding time is the same, high-temperature sintering deformation of the cores obtained by the fully embedded sintering method is the smallest, followed by the half-embedded sintering method, and the largest sintering deformation of the cores obtained by air sintering. When the holding time is 4 h, the air sintering core deformation is 1.6 mm, while the semi-buried sintering is 1.13 mm, while the fully buried sintering is only 0.61 mm. buried powder sintering can reduce the ceramic core in the holding time when the warping deformation is longer, the fully buried sintering anti-warping deformation effect is more obvious. The reason is that the buried powder can provide a uniform temperature field for the core green body during heating, and the sintered powder can provide a support point for the green body, which can reduce the sintering stress and thus reduce the high-temperature sintering deformation of the core.

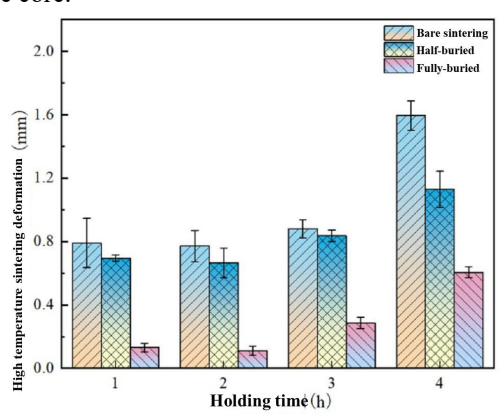


Fig. 7 Effect of holding time on deformation of ceramic cores

3.2.2 Linear shrinkage

The results of linear shrinkage of sintered ceramic cores with different holding times are shown in Fig. 8. Under the same sintering method, the linear shrinkage of

the ceramic core increases gradually with the increase of holding time. When the holding time increases from 1 h to 4 h, the linear shrinkage of ceramic cores increases from 14.36% to 15.78%; semi-buried sintering increases from 12.41% to 14.19%; and fully buried sintering increases from 10.26% to 11.1%. This is due to the increase in linear shrinkage caused by the long time of the ceramic cores in the sintering furnace.

When the holding time was constant, the air sintering linear shrinkage was the largest, followed by semi-buried sintering, and fully buried sintering had the smallest linear shrinkage. When the holding time is 2 h, the linear shrinkage of air-sintered cores is 14.92%, semi-buried sintering is 12.73%, and fully buried sintering is only 10.67%. When the holding time is longer, the ceramic core sintering deformation is larger and the linear shrinkage increases, while the buried powder sintering reduces the sintering deformation and the shrinkage of the ceramic core decreases.

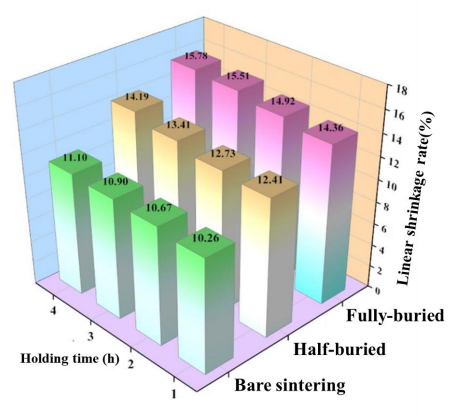


Fig.8 Effect of holding time on X-direction linear shrinkage rate of ceramic cores

3.2.3 Bending strength

The results of the bending strength of sintered ceramic cores with different holding times are shown in Fig. 9. The bending strength of air-sintered cores increases from 2.91 MPa to 4.04 MPa when the holding time is increased from 1 h to 2 h. The bending strength of the cores increases slowly from 4.04 MPa to 4.48 MPa when the holding time is increased from 2 h to 4 h. The bending strength of the cores under half-embedded sintering and fully-embedded sintering methods shows the same trend.

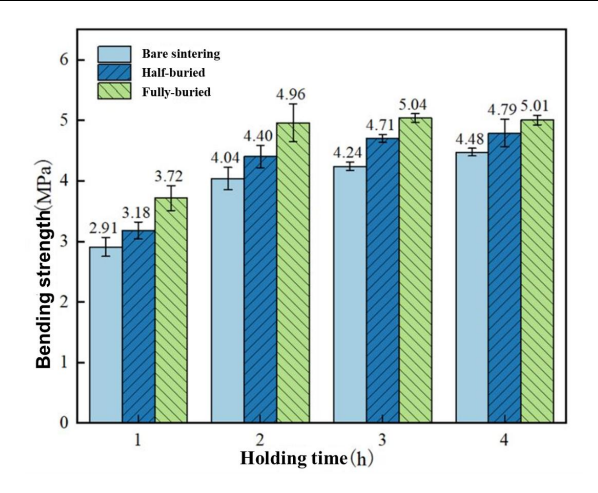


Fig.9 Effect of holding time on flexural strength of ceramic cores

3.2.4 Porosity and bulk density

The porosity of the sintered ceramic cores with different holding times is shown in Fig. 10. When the sintering method is the same, when the holding time is increased from 1 h to 2 h, the bulk density of CaO ceramic cores increases, and when the holding time is increased from 2 h to 4 h, the bulk density of the cores is basically unchanged. While porosity and bulk density and bulk density change trend is opposite, when the holding time increased from 1 h to 4 h, the porosity of ceramic core is the first to decline and then remain unchanged.

When the holding time is the same, the bulk density of ceramic cores with gas sintering method is the largest, followed by half-embedded sintering, and the bulk density of ceramic cores with full-embedded sintering is the smallest. For the porosity, among the three sintering methods, the porosity of fully buried sintered ceramic cores was the largest, followed by semi-buried sintering, and the air sintered ceramic cores had the smallest porosity.

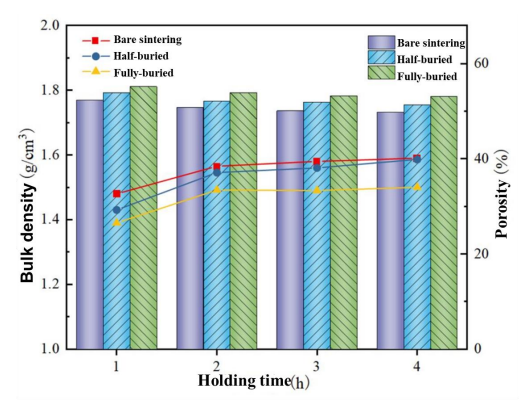


Fig.10 Effect of holding time on porosity and bulk density of ceramic cores

3.2.5 Moisture absorption rate and water solubility rate

The 48-h moisture absorption rates of CaO ceramic cores obtained by sintering at different holding times are shown in Fig. 11. The moisture absorption rates of ceramic cores sintered at different holding times are basically the same, so the holding time has almost no effect on the moisture absorption performance of ceramic cores.

In order to investigate the effect of different sintering methods on the moisture absorption rate of the cores, the moisture absorption rate of ceramic cores with a holding time of 2 h was tested under air, half-buried and full-buried sintering for 48 h. The moisture absorption rate of ceramic cores with a holding time of 2 h was tested as shown in Fig. 12. In the first 12 h, the air-sintered ceramic cores had the largest moisture absorption rate, followed by semi-buried sintering, and the fully buried sintered cores had the smallest moisture absorption rate, and in the 12-48 h period, the fully buried sintered cores had the largest moisture absorption rate, followed by semi-buried sintering, and the air-sintered cores had the smallest moisture absorption rate.

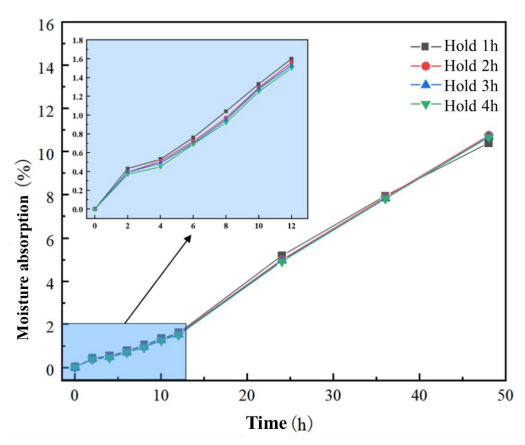


Fig.11 Effect of holding time on moisture absorption rate of ceramic cores

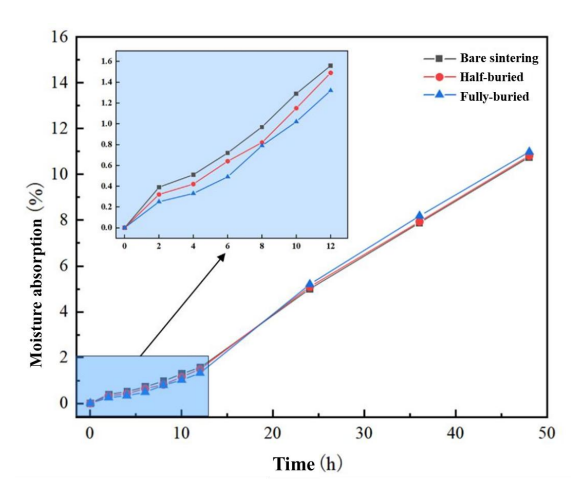


Fig.12 Effect of heating method on moisture absorption rate of

slender ceramic cores

The water dissolution rate of CaO ceramic cores with different holding times is shown in Fig. 13. With the same sintering method, the water dissolution rate of ceramic cores decreases slowly with the increase of holding time, which is due to the increase of holding time increases the bulk density of the cores and decreases the water dissolution rate. When the holding time is the same, air sintered ceramic core water dissolution rate is the fastest, half buried sintering followed by the slowest fully buried sintering. This is due to the buried powder sintering reduces the bulk density inside the core, the larger porosity is conducive to water into the core inside, accelerate the collapse rate of the core, water solubility rate increases.

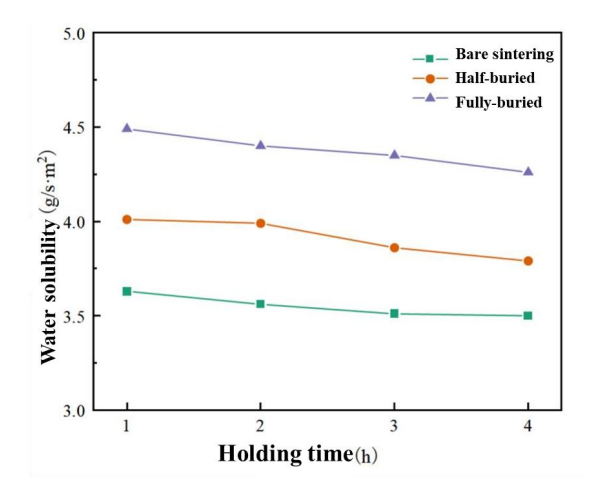


Fig.13 Effect of holding time on water-soluble rate of ceramic cores

3.3 Microscopic morphology analysis

The microscopic morphology of CaO ceramic cores with different holding times is shown in Fig. 14. When the holding time is increased from 1 h to 2 h, the grain density increases and the connection becomes more compact, and with the further increase of the holding time to 3-4 h, the CaO grains are almost no longer further densified.

Holding time is a key stage in the sintering process, and the growth of ceramic particles is mainly in the holding stage. When the holding time reaches a certain length, the ceramic particles do not grow, and the bulk density of the ceramic core does not grow further with the increase of the holding time, so the holding time of 2 h can be used to obtain the densification of the core as well as save the cost of core preparation.

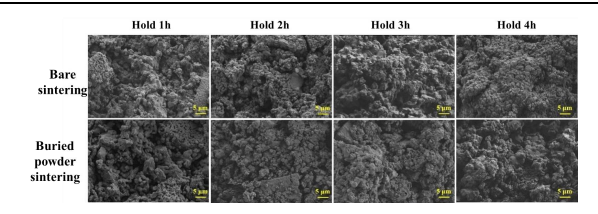


Fig.14 Microscopic morphology of ceramic cores sintered at different holding times

Under the fully buried sintering process, when the holding time is 2 h, the ceramic core does not produce cracks, the thermal deformation is only 0.11 mm, the linear shrinkage is 10.67%, and the bending strength is 4.96 MPa, which reduces the cost and at the same time can get the CaO ceramic cores with excellent comprehensive performance.

4 Conclusions

- Insulation time on the slender ceramic core deformation and cracks do not have a greater impact, with the increase in insulation time, ceramic core bulk density first increased and then remain unchanged, but the insulation time is too long will cause shrinkage and deformation increase.
- The use of buried powder sintering will increase the density of the surface layer of the core, improve the strength; can reduce the bulk density of the inner core, the porosity increases, CaO ceramic core water solubility rate is accelerated, which is conducive to post-casting cleanup.
- Comprehensive consideration of CaO ceramic core sintering deformation, bending strength and water solubility rate and other properties, when the use of industrial alumina buried sintering method, the sintering temperature of 1300 °C, the heating rate of 2 °C / min, the holding time of 2 h, sintered slender CaO ceramic cores have no crack, sintering deformation of only 0.11 mm, linear shrinkage rate of 10.67%, bending strength of 4.96 MPa, the water solubility rate of 4.96 MPa, the water solubility rate of 4.96 MPa, the water solubility rate of 4.96 MPa, and the water dissolution rate was 4.4 g/s·m², with excellent comprehensive performance.

Acknowledgments

National Key Research and Development Program topic projects (No. 2023YFB4605603 and No. 2022YFB4602502). Top project of Natural Science Foundation of Guangdong Province Basic and Applied Basic Research Fund (No. 2024A1515013258). Funded by Shenzhen Science and Technology Program (No. JCYJ20240813114009013). National Natural Science

Foundation of China (No. 52375395). Shenzhen Basic Research Key Program (No. JCYJ20220818102601004). Central Guided Local Science and Technology Development Funds for Free Exploration Category Basic Research Project (No. 2021Szvup158). China University of Geosciences (Wuhan) Teaching Laboratory Open Fund Program (No. SKJ2023125 and No. SKJ2024121). Project funded by the Fundamental Research Operating Expenses of the Central Universities of China University of Geosciences (Wuhan) (No. 2024XLB25 and No. 2024XLB26). National Student Innovation Entrepreneurship Training Program Project (No. 202410491047, No. 202410491048, No. 202410491058, S202410491017, No. S202410491102, X202410491055).

Conflicts of interest:

The authors declare that they have no known competing financial interests or personal relationships that could have appeared to influence the work reported in this paper.

References

- [1] Rahul K, Zhang D, Zhu Qi, et al. Newtonian liquid-assisted material extrusion 3Dprinting: Progress, challenges and future perspectives[J]. Additive Manufacturing, 2024, 79(6): 103903
- [2] Niu Y, Jiang W, Yang L, et al. Preparation of low-cost high strength soluble ceramic cores using heavy calcium carbonate by binder jetting and vacuum impregnation[J].Journal of the European Ceramic Society, 2023, 43: 7714-7720.
- [3] Dadkhah M, Tulliani J, Saboori A, et al. Additive manufacturing of ceramics: Advances, challenges, and outlook[J]. Journal of the European Ceramic Society, 2023, 43(15), 6635-6664.
- [4] Larson N M, Mueller J, Chortos A, et al. Rotational multimaterial printing of filaments with subvoxel control[J]. Nature, 2023, 613(7945): 682-688.
- [5] Pu Q, Jia Z, Kong Y, et al. Microstructure and mechanical properties of 2195 alloys prepared by traditional casting and spray forming[J]. Materials Science and Engineering: A, 2020, 784: 139337.
- [6] Han K H, Baek J W, Lim T W, et al. Digital transformation of metal casting process using sand 3D printing technology with a novel methodology of casting design inside a core[J]. International Journal of Metalcasting, 2023, 17(4): 2674-2679.
- [7] An X, Mu Y, Chen J, et al. Compositional optimization of high-solid-loading ceramic cores via 3D printing[J]. Additive Manufacturing, 2022, 58: 103054.
- [8] Ozkan B, Sameni F, Goulas A, et al. Hot ceramic lithography of silica-based ceramic cores: The effect

- of process temperature on vat-photopolymicrisation[J]. Additive manufacturing, 2022, 58: 103033.
- [9] Zheng W, Wu J M, Chen S, et al. Fabrication of high-performance silica-based ceramic cores through selective laser sintering combined with vacuum infiltration[J]. Additive Manufacturing, 2021, 48: 102396.
- [10] Zhang C, Liu F, Mu Y, et al. High-strength, high-porosity and low-shrinkage Al₂O₃ ceramics prepared by flexible adjustment of CaCO₃ size and content[J]. Journal of the European Ceramic Society, 2024, 44(4): 2304-2316.
- [11] Li Q, An X, Liang J, et al. Balancing flexural strength and porosity in DLP-3D printing Al₂O₃ cores for hollow turbine blades[J]. Journal of Materials Science & Technology, 2022, 104: 19-32.
- [12] Ngo T D, Kashani A, Imbalzano G, et al. Additive manufacturing (3D printing): A review of materials, methods, applications and challenges[J]. Composites Part B: Engineering, 2018, 143: 172-196.
- [13] Wei Y, Gu S, Fang H, et al. Properties of MgO transparent ceramics prepared at low temperature using high sintering activity MgO powders[J]. Journal of the American Ceramic Society, 2020, 103(9): 5382-5391.
- [14] Liu J, Li Y, Yin B, et al. Novel magnesium borate ceramic matrix composites with glass fiber reinforcement[J]. Ceramics International, 2023, 49(7): 11197-11203
- [15] Mu Y, Liu F, Zhang C, et al. Fabrication of high-strength and anti-hydration water-soluble calcia-based ceramic core modified with nano-ZrO₂ via direct ink writing method[J]. Ceramics International, 2023, 49(23): 38623-38634.
- [16] Yang L, Feng Q, Tang S, et al. Effect of CaTiO3 on sintering properties of Y2O3 -based ceramic shell via extrusion-based 3D printing for titanium alloy casting[J].Ceramics International, 2023, 49(11): 19338-19345
- [17] Huang J, Liu F, Han G, et al. Superior comprehensive performance CaO-based core achieved by optimizing particle gradation via orthogonal experiments[J]. International Journal of Applied Ceramic Technology, 2025, 22(1): e14853.
- [18] Li Z, Li J, Luo H, et al. Direct ink writing of 3D piezoelectric ceramics with complex unsupported structures[J]. Journal of the European Ceramic Society, 2022, 42(9): 3841-3847.
- [19] Cipollone D, Mena J A, Sabolsky K, et al. Coaxial Ceramic Direct Ink Writing on Heterogenous and Rough Surfaces: Investigation of Core—Shell Interactions[J]. ACS Applied Materials & Interfaces, 2022, 14(21): 24897-24907.
- [20] Zhao Z. Review of non-destructive testing methods for defect detection of ceramics[J]. Ceramics International, 2021, 47(4): 4389-4397.

- [21] Li H, Liu Y, Liu Y, et al. Effect of burying sintering on the properties of ceramic cores via 3D printing[J]. Journal of Manufacturing Processes, 2020, 57: 380-388.
- [22] Huang L, Long Y, Lin H T, et al. Enhancement of mechanical properties of Os_{0.9}Re_{0.1}B₂ ceramics via buried boron powder assisted sintering[J]. Ceramics International, 2019, 45(12): 14756-14760.
- [23] Xu S Z, Yuan Q Y, Tang Z F, et al. A deformation prediction based on deep learning for sintering process of ceramic core[J]. Advances in Manufacturing, 2025: 1-15.
- [24] Li H, Liu Y, Colombo P, et al. The influence of sintering procedure and porosity on the properties of 3D printed alumina ceramic cores[J]. Ceramics International, 2021, 47(19): 27668-27676.
- [25] Kalemtas A, Topates G, Aytekin Aydin M T, et al. Starch consolidation of SiC ceramics: processing and low-temperature sintering in an air atmosphere[J]. Journal of Asian Ceramic Societies, 2020, 8(1): 106-115.
- [26] Rueschhoff L, Costakis W, Michie M, et al. Additive manufacturing of dense ceramic parts via direct ink writing of aqueous alumina suspension[J]. International Journal of Applied Ceramic Technology, 2016, 5(13): 821-830 Jia Y, Yang J, et al. Enhancing Energy Storage Performance of 0.85 Bi_{0. 5}Na_{0. 5}TiO₃-0.15 LaFeO₃ Lead-Free Ferroelectric Ceramics via Buried Sintering[J]. Materials, 2024, 17(16): 4019.

- Borah K. Dielectric Studies [27] Dutta nano-magnesium silicate and linear low-density polvethylene composite as a substrate high-frequency applications[J]. Journal of Electronic Materials, 2022, 51(9): 5368-5375.
- [28] Tang S, Yang Y, Fan Z, et al. A novel composite binder design for direct ink writing alumina-based ceramics with enhanced strength at low sintering temperature[J]. Ceramics International, 2022, 48(6): 7963-7974.
- [29] Baltazar J, Torres P M C, Dias-De-Oliveir J, et al. Influence of filament patterning in structural properties of dense alumina ceramics printed by robocasting[J]. Journal of Manufacturing Processes, 2021, 68: 569-582.
- [30] Del-Mazo-Barbara L, Ginebra M. Rheological characterisation of ceramic inks for 3D direct ink writing: A review[J]. Journal of the European Ceramic Society, 2021,41(16): 18-33.
- [31] Kwon S Y, Jung I. Critical evaluation and thermodynamic optimization of the CaO-ZrO2 and SiO2-ZrO2 systems[J]. Journal of the European Ceramic Society, 2017,37(3): 1105-1116.
- [32] Michel D. A probabilistic rate theory connecting kinetics to thermodynamics[J]. Physica A: Statistical Mechanics and its Applications, 2018, 503: 26-44.
- [33] Kong D, Guo A, Hu Y, et al. Alumina-based ceramic cores prepared by vat photopolymerization and buried combustion method[J]. Materials Today Communications, 2023, 37(6):107434.